Experimental Neurology 299 (2018) 15–25

Contents lists available at ScienceDirect

Experimental Neurology

journal homepage: www.elsevier.com/locate/yexnr

Research Paper

Reversible induction of TDP-43 granules in cortical neurons after traumatic injury

Diana Wiesner[a], Lilla Tar[a], Birgit Linkus[a], Akila Chandrasekar[a], Florian olde Heuvel[a], Luc Dupuis[b,c], William Tsao[d,e], Philip C. Wong[d,e,f], Albert Ludolph[a], Francesco Roselli[a,g,*]

[a] Dept. of Neurology, University of Ulm School of Medicine, Ulm, Germany
[b] Inserm U1118, Mécanismes centraux et périphétiques de la neurodégénérescence, Strasbourg, France
[c] Université de Strasbourg, Faculté de Médecine, Strasbourg, France
[d] Dept. of Pathology, Johns Hopkins University School of Medicine, Baltimore, MD, United States
[e] Cellular and Molecular Medicine Program, Johns Hopkins University School of Medicine, Baltimore, United States
[f] Department of Neuroscience, Johns Hopkins University School of Medicine, Baltimore, United States
[g] Dept. of Anatomy and Cell Biology, University of Ulm School of Medicine, Germany

ARTICLE INFO

Keywords:
TDP-43
Cortical injury
ALS

ABSTRACT

Traumatic brain injury (TBI) has been proposed as a risk factor for neurodegenerative diseases, including amyotrophic lateral sclerosis (ALS). To determine whether TBI might trigger or exacerbate ALS-relevant pathology, we delivered a mild stab-wound injury to the motor cortex of three different ALS mouse models expressing mutations in SOD1, TDP-43 or FUS and scrutinized the effects on the formation of phospho-TDP-43 (pTDP-43) cytoplasmic granules. Stab-injury induced the formation of cytoplasmic TDP-43 granules in wt animals, peaking at 3 dpi; a much larger response was seen in mutant TDP-43 mice, whose response peaked at 7 dpi. The pTDP-43 granules did not colocalize with the stress markers TIAR-1 and FUS but colocalized with FMRP (35%) and with p62 (65%), suggesting their involvement in transport granules and their clearance by autophagy. A similar, albeit smaller effect, was seen in mutant FUS mice. In the SOD1^{G93A} mouse model, neither increase in pTDP-43 granules nor in SOD1 aggregates were detected. In all cases, pTDP-43 granules were cleared and the number of pTDP-43-positive neurons returned to baseline by 40 dpi. Neither injury-related neuronal loss nor motor performance or survival was significantly different in transgenic mice receiving injury vs sham mice. Thus, trauma can trigger ALS-related TDP-43 pathology, the extent of which is modulated by ALS-related mutations. However, the pathological findings prove reversible and do not affect disease progression and neuronal vulnerability.

1. Introduction

Amyotrophic lateral sclerosis is the most common human adult motor neuron disease, characterized by an onset in the sixth-seventh decade and a progressive course of 4–5 years on average (Caller et al., 2015; Couratier et al., 2016). Up to 20 mutated genes are currently known to be causally linked to the disease (Hübers et al., 2015; Freischmidt et al., 2015; Brenner et al., 2016; Riva et al., 2016). The majority of ALS patients does not carry mutations in known ALS-related genes and it is thought that causative environmental factors contribute to sporadic ALS, either on their own or, most likely, on the top of a background of genetic susceptibility (Steinberg et al., 2015; Xi et al., 2014). Notably, a majority of both sporadic and genetic cases display aggregates of TDP-43 and FUS, whose mutations are causally linked to ALS (Neumann et al., 2009; Urwin et al., 2010).

Traumatic brain injury (head trauma in general) has been repeatedly (yet controversially) associated with motor neuron disease, based on epidemiological and neuropathological evidence. High ALS incidence in professional soccer and football players (Chiò et al., 2005; Lehman et al., 2012) suggests that subclinical lesions of the grey matter may be involved in triggering pathogenic cascades related to ALS or FTD (Wang et al., 2015). Indeed, chronic traumatic encephalopathy, a degenerative brain disease found in athletes, was associated with TDP-43 deposition, a hallmark of ALS pathobiochemistry (McKee et al., 2010; Brettschneider et al., 2013; Brettschneider et al., 2014). In TBI brain samples, increased immunoreactivity for TDP-43 (but not pathological inclusions) has been established (Johnson et al., 2011). Traumatic damage (Rosenbohm et al., 2014) or arteriovenous

* Corresponding author at: Dept. of Neurology, University of Ulm-School of Medicine, Center for Biomedical Research, Helmholzstrasse 8/2, 89081 Ulm (DE), Germany.
E-mail address: francesco.roselli@uni-ulm.de (F. Roselli).

http://dx.doi.org/10.1016/j.expneurol.2017.09.011
Received 12 May 2017; Received in revised form 18 August 2017; Accepted 19 September 2017
Available online 21 September 2017

malformations (Valavanis et al., 2014) of the primary motor cortex have also been associated with risk for ALS. According to a case study, head trauma could also have triggered the appearance of the disease in only one of two monozygous twins both carriers of the *C9ORF72* expansion but being discordant for clinical phenotype (Xi et al., 2014). However, the relationship between head trauma and ALS was not observed in a large Swedish cohort (Peters et al., 2013) and previous head injury did not increase the rate of progression in ALS patients (Fournier et al., 2015). A meta-analysis of several studies was inconclusive (Armon and Nelson, 2012). Therefore, it remains controversial whether traumatic brain injuries, in particular motor cortex injuries, affecting pre-symptomatic gene-carriers may constitute a triggering factor for ALS-related pathology and lead to the manifestation of the disease.

In this study, we set out to investigate whether a controlled damage to primary motor cortex in murine models of ALS (SOD1, TDP-43, FUS), delivered before the appearance of degenerative symptoms, could trigger ALS-related pathobiochemisty and lead to an earlier onset or an accelerated progression of the motor impairment.

2. Materials and methods

2.1. Animals

All procedures were performed in agreement with the local and national animal welfare legislation, under permit no. 1214 and permit no. 1222. Transgenic TDP-43^{G298S} mice, transgenic SOD1^{G93A} mice and FUS$^{\Delta NLS/+}$ mice were maintained and genotyped as described (Scekic-Zahirovic et al., 2016; Gurney et al., 1994). Transgenic TDP-43^{G298S} mice will be object of a detailed independent publication and were obtained with the same approach as previously reported (Shan et al., 2010) using the Thy1 promoter to drive the expression of mutant human TDP-43. Mice were maintained at 22 °C with a 14/10 h light/dark cycle and had food and water ad libitum. Mice were regularly monitored to assess onset and progression of symptoms and were considered to be at end stage when they were not able to right themselves immediately when placed on their side. For histological analysis, animals were deeply anesthetized with 1 mg/kg body weight ketamine chlorhydrate and 0.5 mg/kg body weight xylazine, and transcardially perfused with 4% paraformaldehyde in 0.1 M pH 7.4 phosphate buffer. After perfusion, the tissue was dissected quickly, post-fixed for 24 h in 4% paraformaldehyde and cryoprotected for 48 h in 30% sucrose in PBS. Brains were then embedded in tissue tek before cryostat sectioning.

2.2. Surgical lesion of the primary motor cortex

Experimental lesion to primary motor cortex was performed with the stab-injury protocol previously reported (Buffo et al., 2008) in correspondence with primary motor cortex stereotactic coordinates (+1, +1, −0.8, Paxinos Mouse Brain Atlas). In brief, 60 days old mice were anesthetized with an intraperitoneal injection of midazolam (5 mg/kg of body weight), medetomidine (0.5 mg/kg) and fentanyl (0.05 mg/kg) and a unilateral craniotomy (diameter of 3 mm) was performed 1 mm anterior to the bregma and 1 mm to the right of the midline. For producing a stab-injury, a lancet-shaped knife was inserted into the primary motor cortex, to a depth of 0.8 mm, and moved 1 mm in a dorsal direction. The craniotomy was covered with a permanent cutaneous suture (Vicryl 4–0 (SH-1 plus)). Anesthesia was antagonized with an intraperitoneal injection of atipamezole (2.5 mg per kg), flumazenil (0.5 mg per kg) and buprenorphine (0.1 mg per kg).

2.3. Weight-drop closed TBI model

The weight-drop TBI model was performed in agreement with published protocol (Flierl et al., 2009). Briefly, B6SJL wt male mice aged 80–90 days were pre-treated with buprenorphine (0.1 mg/kg by subcutaneously injection) and put under sevoflurane anesthesia (2,5% in 97,5% O_2). The scalp skin was incised on the midline to expose the skull. Animals were then manually positioned in the weight-drop apparatus, as previously described, with the impactor site localized at the center of the right parietal bone. TBI was delivered by a 333 g impactor free-falling from a 2 cm distance. After the weight drop, animals were administered 100% O_2 and monitored for the apnea time. Once spontaneous breathing was restored, the scalp skin of the anesthetized mice was stitched with Prolene 6.0 surgical thread and the animals were transferred to a warmed recovery cage (single-housed) with ad libitum access to food and water. Additional doses of buprenorphine were administered every 12 h for the following 24 h post-injury. To avoid unnecessary suffering of the mice, their general state was checked regularly using a score sheet developed for TBI, determining (NSS score) fixed termination criteria. Effort was made to minimize animal suffering and reduce the number of required animals.

2.4. Behavioral testing

Starting at the age of 3 weeks, male mice were put into the running wheel cages and handled every day. Motor performance was recorded every night, during the dark phase for 10 h. Once per week, starting at the age of 4 weeks, body weight, inverted grid test and grip strength (forelimbs only and all-four limbs) were assessed for each transgenic and wild type mouse. Grip strength measurements were done using a grip strength meter (Bioseb gripmeter, Vitrolles, France). Each measurement was performed in triplicates and data were averaged. The inverted grid was performed to measure the muscular strength and motor coordination of the mice (van Putten et al., 2010). The mouse was placed on the grid and the grid was turned. The time was recorded from the turning of the grid till the mouse fell down (maximum of 300 s hanging time).

2.5. Immunohistochemistry

Free floating brain cryosections (40 μm) were prepared and processed according to previously published protocols. Primary antibodies (anti-pTDP-43 [Ser409/410] SIG-39852, Biolegend (1:200); anti TIAR-1, Santa Cruz biotechnology(1:500); anti-FMRP, Abcam (1:200); anti-SQSTM1/p62, Abcam (1:100); FUS/TLS, Proteintech (1:100); B8H10 monoclonal antibody misfolded SOD, MediMabs antibodies, (1:500)) diluted in donkey serum 3%/0.1% TritonX-100 in PBS were incubated overnight at 4 °C. Secondary antibodies (Donkey anti rabbit Alexa Fluor 568, A10042, Life Technologies; donkey anti mouse Alexa Fluor 488, ab150153, Abcam; donkey anti rat Alexa Flour 488, abcam; all 1:1000) were incubated for 2 h at room temperature. Slides were mounted using ProLong® Gold antifade reagent (molecular probes, Life Technologies). For visualizing neurons in the mouse brain NeuroTrace® 435/455 Blue Fluorescent Nissl Stain (N21479, Thermo Fischer Scientific) was used. Images were acquired with a laser scanning microscope (Zeiss 710) equipped with a Plan-Apochromat 63 × oil DIC immersion lens. Images (more-dimensional stacks) were acquired and analyzed using Zeiss ZEN 2010 software and ImageJ 1.44p. Optical stacks containing 20 optical sections, each 0.5 μm thick, were collapsed and used for the analysis of pTDP-43 granules in the cytoplasm. The numbers of pTDP-43$^+$ neurons (neurons with > 3 pTDP-43 granules in the cytoplasm were considered positive) were counted and correlated to the total numbers of neuronal cells. Results are represented as means ± SEM.

2.6. Statistical procedures

For statistical analysis, one-way ANOVA was used for comparing mean values that were considered significantly different. Data are presented as mean ± standard error of the mean (SEM). Graph Prism software (GraphPad Software Inc.) was used to perform statistical analysis.

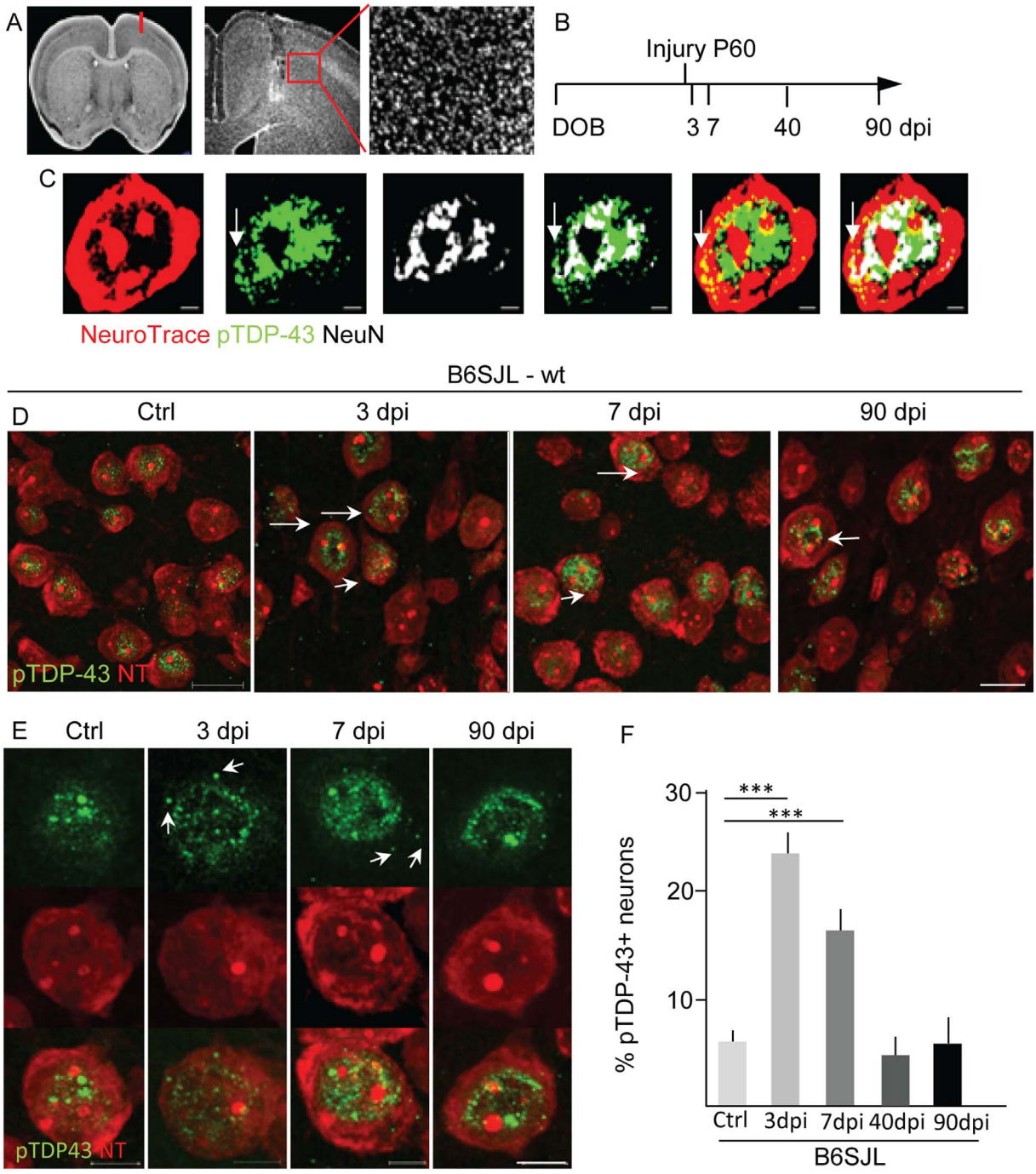

Fig. 1. (A) schematic representation of the surgical lesion to primary motor cortex and stab wound (red line) into layer V (http://www.mbl.org/atlas165/15.html) and analyzed area (layer V) (B) Schematic representation of the experimental design: stab injury was performed at P60 and animals were sacrificed at 3,7,40 and 90 dpi. (C) Immunostaining for NeuN, NeuroTrace and pTDP-43, in order to highlight the nucleus, the cytoplasm and pTDP-43 granules, respectively, reveals the cytoplasmic localization of pTDP-43 granules. (D-E) immunofluorescence images from layer V neurons of wildtype (WT; B6SJL) mice 3, 7 and 90 dpi. (E) Top panel: pTDP-43 granules in the cytoplasm are marked with arrows; middle panel: morphology of layer V neurons labeled with NeuroTrace; bottom panel: merged images of layer V neurons with pTDP-43 granules. Scale bar (D) = 20 μm (C,E) = 5 μm. (F) percentage of pTDP-43 + neurons (layer V neurons that displayed pTDP-43 granules in the cytoplasm); $^{**}p < 0.1$, $^{***}p < 0.001$. (For interpretation of the references to colour in this figure legend, the reader is referred to the web version of this article.)

3. Results

3.1. Focal injury to motor cortex triggers the formation of cytoplasmic pTDP-43 granules in wild type mice

Phosphorylation and translocation to the cytoplasm of TDP-43 are thought to be important steps in ALS pathogenesis, and are known to take place in response to inflammatory stimuli or metabolic stress (Correia et al., 2015; Dewey et al., 2011). Therefore, we tested if the experimental injury to the motor cortex in wild type (wt) animals induced translocation of TDP-43 to the cytoplasm and the formation of phosphorylated, cytoplasmic granules in neurons. To this purpose, we performed a focal mechanical lesion (or sham surgery) in the primary motor cortex (Simon et al., 2011; Buffo et al., 2008) and sacrificed animals 3, 7, 40 and 90 days post injury (dpi) (Fig. 1A, B). Sections encompassing the site of injury in the motor cortex were

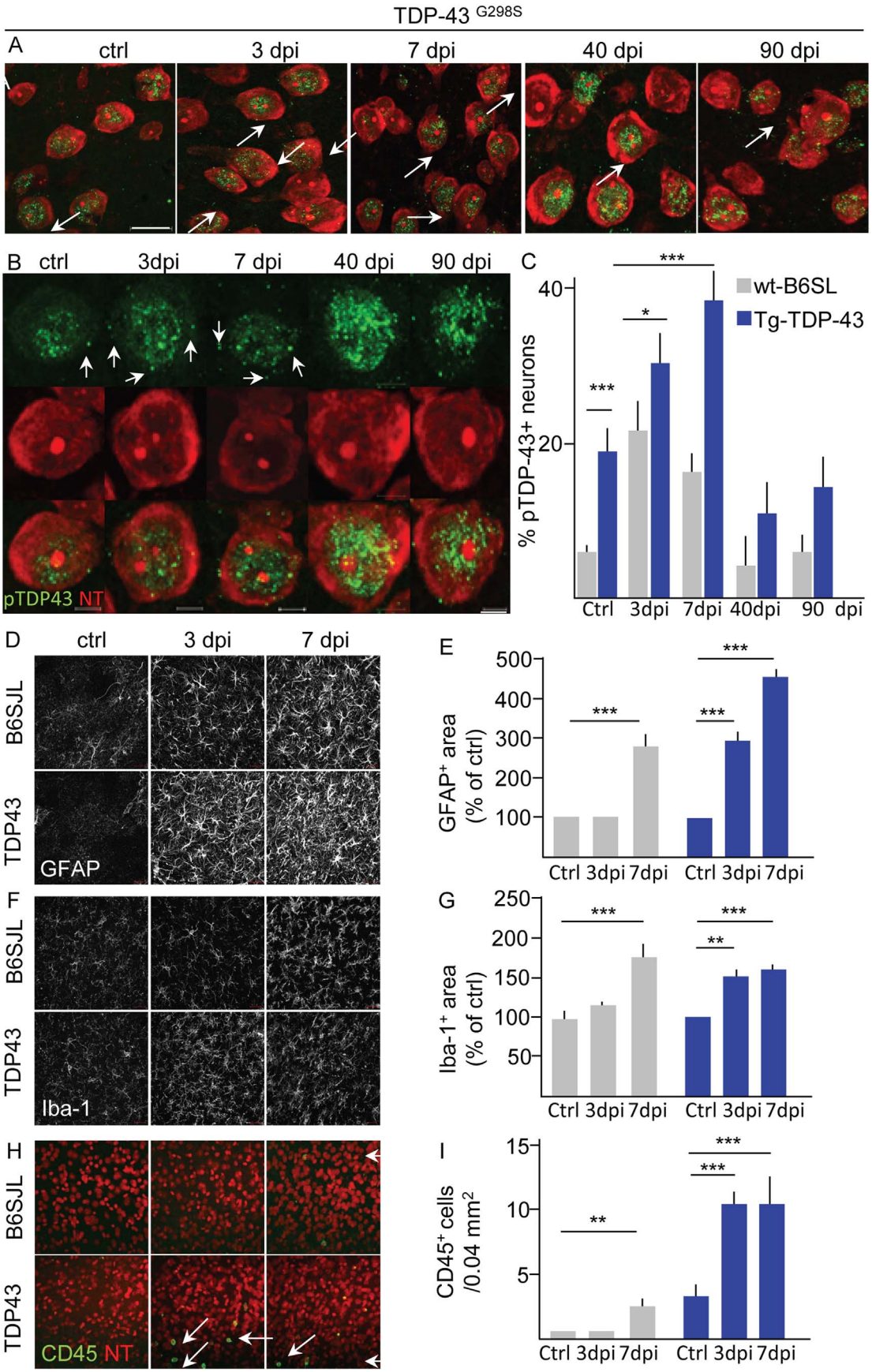

(caption on next page)

Fig. 2. (A,B) immunofluorescence images from layer V neurons of TDP-43^{G298S} mice, 3, 7, 40 and 90 dpi. (B) Top panel: pTDP-43 granules in the cytoplasm are marked with arrows; middle panel: morphology of layer V neurons labeled with NeuroTrace; bottom panel: merged images of layer V neurons with pTDP-43 granules. Scale bar (A) = 20 μm (B) = 5 μm. (C) Percentage of pTDP-43^{+} neurons in wildtype - (WT; B6SJL) and TDP-43^{G298S} mice (TDP-43). (D–E) Immunostaining for the astrocyte marker GFAP reveals increased gliotic response to trauma in TDP-43^{G298S}. (F–G) Microglial response to trauma is comparable in WT and TDP-43^{G298S} mice. (H−I) Leukocytes infiltration (CD45 + cells) upon stab injury is strongly enhanced in TDP-43^{G298S} mice. Scale bar = 20 μm *$p < 0.5$, ***$p < 0.001$.

immunostained with anti-phospho-TDP-43 (together with NeuroTrace® as neuronal marker). Both at 3 dpi and 7 dpi, the nuclear pool of pTDP-43 was substantially preserved and only small granules could be detected in the cytoplasm of a subset of neurons (Fig. 1C). In fact, in control (sham-operated) wild type-mice, about 6% (6.02 ± 1.03%) of neurons in layer V of motor cortex displayed cytoplasmic pTDP-43^{+} granules (henceforth "pTDP-43^{+} neurons"). The number of pTDP-43^{+} neurons were strongly increased 3 days after injury (22.20 ± 3.39% vs 9.92 ± 2.56% in sham controls; $p < 0.01$) and declined slightly at the 7 dpi time point (16.60 ± 2.45% vs 7.74 ± 1.53% in sham controls; $p < 0.01$; Fig. 1D–F).

Notably, pTDP-43 granules were cleared from layer V neurons with time and the percentage of neurons displaying such granules declined to baseline values at 40 dpi (4.55 ± 1.78% of baseline, not shown) and remained at this level at later time point (90 dpi: 6.48 ± 1.81% of pTDP-43^{+} neurons compared to 6% at baseline, $p > 0.05$; Fig. 2C).

Since a stab-injury TBI is exceedingly rare in human patients (although provides high experimental reproducibility), we investigated if a similar effect on pTDP-43 + granules was detectable in mild TBI based on a closed, blunt weight-drop model. Wt mice were subject to a 2-cm weight-drop TBI (according to Flierl et al., 2009) and sacrificed at 3 or 7 dpi. In contrast to stab-injury, major disruptions of the motor cortex (such as tearing of the cortical ribbon) or blood extravasation (traumatic hemorrhage) were not observed in the weight-drop model. Interestingly, neither the number of pTDP-43^{+} neurons nor the burden of pTDP-43 granules per neuron were increased in the weight-drop model (Suppl. Fig. 1), suggesting that a certain degree of tissue disruption is necessary for the induction of pTDP-43 granules.

3.2. Cytoplasmic pTDP-43^{+} granules formation is enhanced in TDP-43^{G298S} and FUS$^{\Delta NLS/+}$ mice

Next, we tested if ALS-related mutations in TDP-43^{G298S} (henceforth "TDP mice") or FUS$^{\Delta NLS/+}$ (henceforth "FUS mice") mice may significantly affect the formation of cytoplasmic pTDP-43^{+} granules in response to traumatic injury.

At baseline, control TDP-43 mice displayed a higher percentage of pTDP-43^{+} neurons than control B6SJL-WT mice (18.23 ± 2.42% vs 6.02 ± 1.03% in wt mice; Fig. 2). After the stab injury, TDP-43 transgenic (tg) mice displayed an increase in pTDP-43^{+} neurons at 3 days compared to baseline (30.65 ± 4.02% vs 18.23 ± 2.42% at baseline, $p < 0.01$; when compared to wt littermates, 22.20 ± 3.39%, $p > 0.05$; Fig. 2A–C) and a further increase at 7 days after the injury (up to 38.37 ± 4.38% pTDP-43^{+} neurons), whereas, pTDP-43^{+} neurons did not decline in wt mice at 7 dpi (16.60 ± 2.45%; Fig. 2C). Notably, the burden of pTDP-43^{+} granules in each neuron (the percentage of volume occupied by granules in the cytoplasm) was not larger in the neurons of injured TDP-43 tg mice when compared to wt mice at any age (not shown).

Interestingly, the percentage of pTDP-43^{+} neurons declined progressively, being comparable at 40 dpi (10.82% ± 1.79%) and 90 dpi with baseline TDP-43 tg mice (still higher than in wt animals: 16.37 ± 2.79% vs 6.48 ± 1.81%; $p < 0.001$).

On the other hand, the percentage of pTDP-43^{+} neurons was comparable in control FUS mice and control C57BL/6 Tac-wt mice (0.56 ± 0.42% in control FUS mice compared to 1.10 ± 0.53% in control wt mice; Fig. 4). However, the absolute values of pTDP-43^{+} neurons in C57BL/6 Tac-wt mice were significantly lower when compared to control wt mice of a different genetic background (1.10 ± 0.53% in C57BL/6 Tac compared to 6.02 ± 1.03% in B6SJL). Three days after injury neither FUS mice nor their wt controls displayed a significant increase in pTDP-43^{+} neurons. However, at 7 dpi the percentage of pTDP-43^{+} neurons were slightly increased in wt mice (1.80 ± 0.72%, as compared to 1.00 ± 0.69% in control mice and 0.88 ± 0.62% at 3 dpi) but strongly augmented in FUS mice (3.62 ± 1.31% compared to 0.37 ± 0.37% at 3 dpi; $p < 0.05$ when compared to the 7 dpi wt and to 3 dpi wt or FUS). Similar to what is observed in TDP-43 tg mice, the percentage of pTDP-43^{+} neurons decreased to baseline at the 90 dpi (when it was no longer different from wt littermates).

3.3. Cytoplasmic pTDP-43^{+} granules constitute a heterogeneous population partially colocalizing with RNA binding proteins and autophagy markers

TDP-43 takes part in the composition of several RNA-processing granules, together with several other RNA-binding proteins. In order to detail the nature of the pTDP-43 granules, we performed double-immunostaining for pTDP-43 and for the RNA-binding proteins TIAR1, FUS and FMRP or for the autophagy marker p62 in cortical samples from *TDP-43^{G298S}* mice at 7 dpi. Interestingly, only 4.25 ± 2.10% of pTDP-43 granules was also positive for the stress-granules marker TIAR1 (Fig. 3A,E) and only 6.05 ± 1.35% of pTDP-43 granules was immunopositive for FUS (Fig. 3D,E). Notably, 39.17 ± 5.46% of pTDP-43 granules were immunopositive for FMRP (Fig. 3B,E), suggesting that they may belong to the family of transport RNA granules (Dictenberg et al., 2008; Coyne et al., 2015). However, 58.17 ± 5.37% of pTDP-43 granules colocalized with the autophagy marker p62 (Fig. 3C,E), implying that, irrespective of their original identity, the majority of pTDP-43 granules were targeted for autophagy.

Thus, the pTDP-43 granules induced by the stab-injury appear to be heterogeneous and, for substantial fraction, part of the transport granules group but not of the stress-granules group; furthermore, they appear to be undergoing autophagic degradation.

3.4. Enhanced astrocytes and leukocytes response to stab injury in TDP-43^{G298S} mice

The neuroinflammatory activation is both a hallmark of the pathogenic cascade set in motion by TBI and is a critical component of the non-cell-autonomous pathways in ALS (Gyoneva et al., 2015; Philips and Robberecht, 2011). Therefore, we explored if the different inductions of neuronal pTDP-43 pathologies were mirrored in the differential activation of glial cells (Fig. 2D–E). In wt mice, the stab injury resulted in the activation of astrocytes (as detected by the increased coverage of GFAP^{+} processes) at 7 dpi (287.28 ± 22.49% of baseline, $p < 0.001$) but not at 3 dpi (108.30 ± 2.99% of baseline, $p > 0.05$; Fig. 2D–E). Surprisingly, in TDP-43^{G298S} mice, the response of astrocytes was already strongly detectable at 3 dpi (297.40 ± 17.29% of baseline, $p < 0.001$) and was significantly larger at 7 dpi (455.30 ± 16.30% of baseline, $p < 0.001$; Fig. 2D–E).

Likewise, microglial activation (as shown by Iba-1 staining) was markedly increased at 3 dpi in TDP-43^{G298S} mice when compared to wt mice (159.70 ± 3.28% of baseline in TDP-43 ^{G298S} mice, vs 105.4 ± 3.3% in wt littermates, $p < 0.01$; Fig. 2F–G) but became comparable at 7 dpi (166.70 ± 3.20% vs 173.35 ± 6.5%, $p > 0.05$; Fig. 2F–G).

Finally, we monitored the appearance of CD45^{+} cells (highlighting the infiltration of leukocytes). Wt mice displayed a modest increase in CD45 + cells at 3 and 7 dpi (3 dpi: 0.1 ± 0.04/0.04mm^2; 7 dpi: 2.75 ± 0.48/0.04 mm^2); on the other hand, TDP-43^{G298S} mice showed

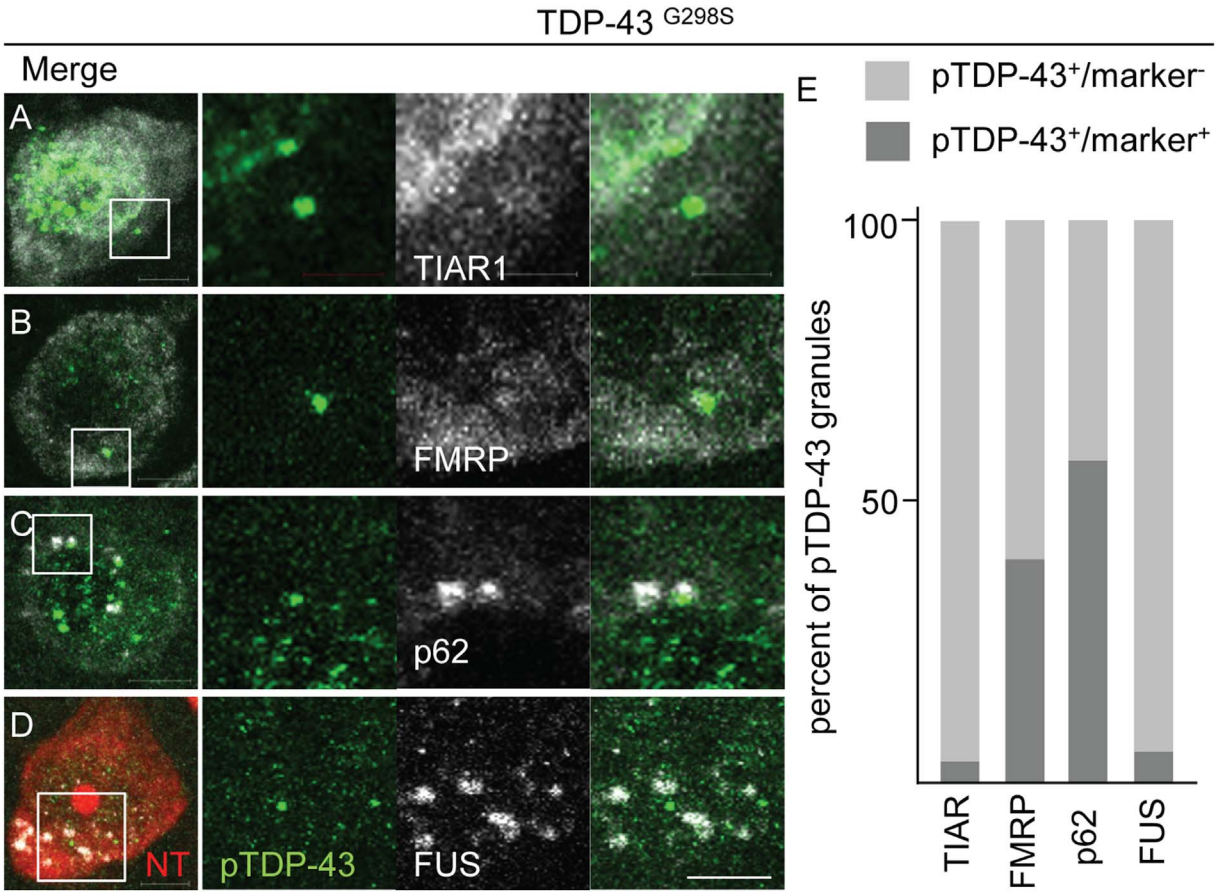

Fig. 3. Colocalization of pTDP-43 granules with stress granules markers TIAR1 (A), FUS (D), transport granules FMRP (B) and autophagy structures p62 (C) reveals that although only 5% (quantification in E) of pTDP-43 granules are stress granules, a large fraction (about 35%) belongs to the transport granules group and that the majority (65%) may be involved in autophagic degradation. Scale bar = 5 μm.

a four-fold increase in CD45 + cells (compared to wt) at 3 dpi and at 7 dpi (3 dpi: 10.0 ± 1.47/0.04mm^2; 7 dpi: 10.5 ± 2.1/0.04mm^2; both $p < 0.01$ vs wt; Fig. 2H–I).

Thus, the glial and inflammatory reaction to TBI was significantly more pronounced in TDP-43^{G298S} mice, despite the neuronal-restriction to the expression of the transgene.

3.5. Cytoplasmic pTDP-43$^+$ granules formation is not increased in low-copy SOD1^{G93A} transgenic mice

We then proceeded to analyze injury-induced pTDP-43$^+$ granule formation in the low-copy (i.e., slow progressing) SOD1^{G93A} transgenic mouse (henceforth, SOD1 mice; Gurney et al., 1994). At baseline, the number of pTDP-43$^+$ neurons was comparable between control B6SJL-wt and control SOD1 mice. Surprisingly, mild stab wound TBI did not lead to an increase of pTDP-43$^+$ neurons in SOD1 mice at any time point tested, with the values remaining at (or even below) baseline (Fig. 5).

Notably, we detected a significant effect of the background strain in the pTDP-43 response after traumatic injury: C57BL/6 Tac (wildtype to FUS) mice (Suppl. Fig. 2): showed a number of pTDP-43$^+$ neurons at baseline as well as at 3 and 7 dpi which was significantly larger than what was observed in B6SJL (wild type to TDP-43 and SOD1; at baseline, 6.02 ± 1.03% vs 1.10 ± 0.53%, $p < 0.001$).

Finally, we verified whether, despite not increasing TDP-43 pathology, TBI could trigger the increase of the burden of misfolded SOD1 pathology. To this aim, we immunostained cortical sections spanning the injury site with the misfolded-SOD1-specific monoclonal antibody B8H10 (Pickles et al., 2013). Cytoplasmic aggregates positive for misfolded SOD1 could be detected both in sham and in TBI samples. At 7 dpi, there was no difference in the number of misfSOD1$^+$ neurons and the burden of misfSOD1 in positive neurons (SOD1 sham vs SOD1 + TBI: 42.00 ± 5.69% vs 53.68 ± 6.49%). Both sham and TBI mice displayed a marked increase in the number of misfSOD1$^+$ neurons at 90 dpi but also at this age also there was no difference between the two groups (SOD1 sham vs SOD1 + TBI: 85.86 ± 7.29% vs 84.65 ± 3.90%; Fig. 5D–E).

Thus, in the SOD1(G93A) mouse model, TBI did not affect the appearance of TDP-43 or SOD1 pathology.

3.6. Dose-dependent effect of injury on formation of pTDP-43 granules

Since the pathological consequences of the injury may non-linearly depend on the extent of the damage, we compared two injury models in wt and TDP-43 tg mice: a single linear cut in the motor cortex ("simple injury") and three parallel cuts, spaced 200 μm, in the same site (extended injury) (Fig. 6).

In wt mice, the extended injury caused a significant increase in the percentage of pTDP-43$^+$ neurons at the 3 dpi (up to 31.56 ± 3.15% vs. 22.20 ± 3.39% in simple injury and at the 7 dpi (34.22 ± 3.54% vs. 16.60 ± 2.45% in simple injury) time points. At 90 days, the percentage of pTDP-43$^+$ neurons were similar in both wt groups (extended: 11.39 ± 2.24% vs simple: 6.48 ± 1.81%), reaching baseline levels.

However, when simple and extended injury models were applied to the TDP-43 tg mice, the extended injury did not cause any further increase in the percentage of pTDP-43$^+$ neurons at 3 days after injury compared to the simple injury (30.31 ± 2.65% vs simple

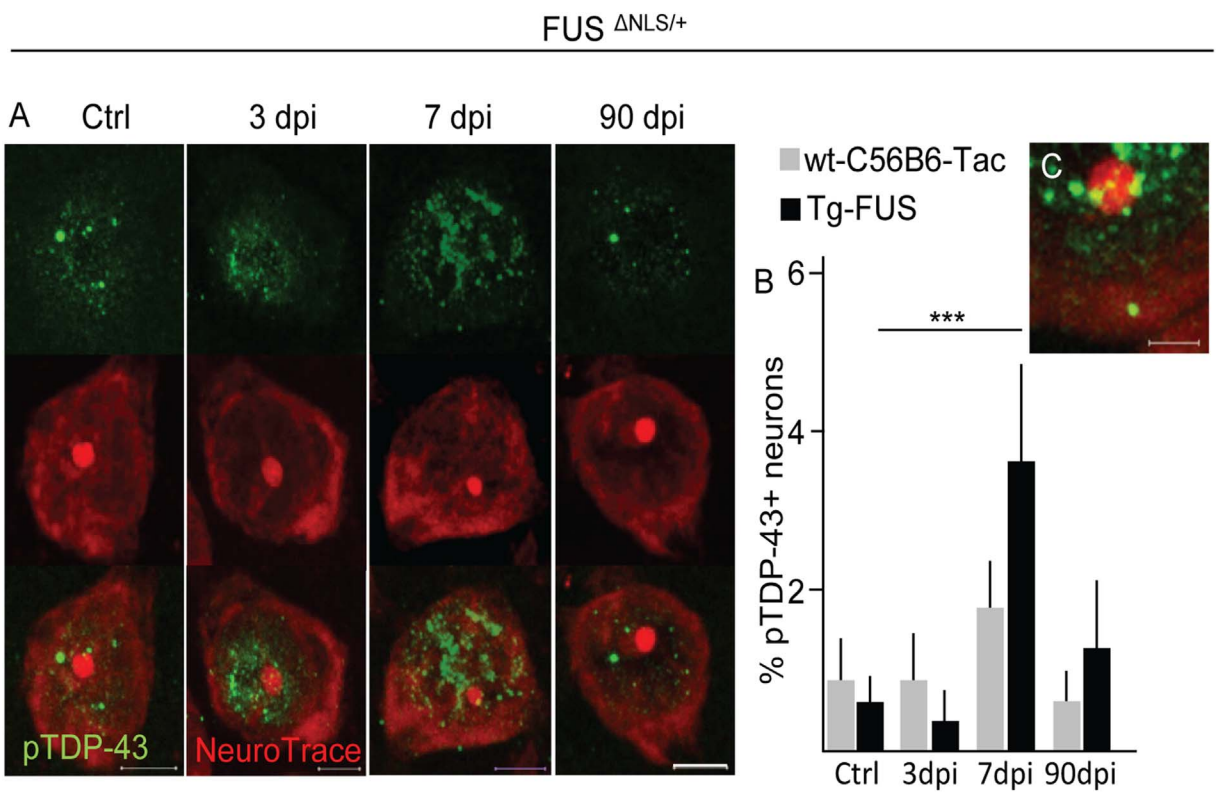

Fig. 4. Delayed appearance of pTDP-43 granules in FUS$^{\Delta NLS/+}$ mice (A–B) Immunofluorescence images from layer V neurons of, 3, 7 and 90 dpi show that pTDP-43 granules only appear at 7 dpi but not at 3 dpi in mutant FUS mice. Scale bar = 5 μm. *$p < 0.5$. (C) immunofluorescence image of TDP-43 granules outside the nucleus at higher magnification (FUS$^{\Delta NLS/+}$ 7 dpi), Scale bar = 2 μm.

30.65 ± 4.02%). On the other hand, at 7 dpi, extended injury TDP-43 tg mice displayed a significant increase (up to 53.01 ± 2.91%, vs 38.37 ± 4.38% in the simple injury group) in the percentage of neurons displaying cytoplasmic pTDP-43^{+} granules. Finally, at 90 dpi, the percentage of pTDP-43^{+} neurons in TDP-43 tg mice which underwent simple injury or extended injury was almost equal (simple 16.37 ± 2.79% vs extended 10.93 ± 2.42%). The burden of pTDP-43^{+} granules in each positive neuron was comparable between the extended injury group and the simple injury group at all time points analyzed, indicating that a more severe lesion increases only the number of affected neurons but not the amount of cytoplasmic pTDP-43 granules.

3.7. Neuronal viability and long-term motor performance after stab injury is not worsened in ALS mouse models

The severity of the injury (stab size and location) was highly reproducible in all mice that underwent stab wound injury. The overall number of cortical neurons in a volume of interest located in layer V, medial to the injury, was not significantly lower, at 3, 7 or 90 dpi, in TDP-43, FUS or SOD1 mice when compared to control or to the corresponding wt mice (Suppl. Fig. 3 and data not shown), implying that the different mutations, although pathogenic for the development of ALS/FTD, did not increase the vulnerability to traumatic injury.

Finally, we examined the long-term consequences of traumatic brain injury in the context of different genetic backgrounds and mutation status. Despite the prominent response in terms of pTDP-43^{+} granule formation, neither acute nor long-term effects on motor performance were detected in both wt strains or in the TDP-43 or in the SOD1 transgenic line (because of the lack of TBI effect on TDP-43 and SOD1 mice, of the limited effect on pTDP-43 granules in the FUS mice and given the absence of overt phenotype in this line, as shown in Supplementary Fig. 5, a full analysis any of the effect of TBI on FUS mice motor performance was not performed in order to avoid unnecessary suffering of experimental animals, according to current regulation). In particular, the progression of the impairment of grip strength and motor activity in the running-wheel test were comparable between control and TBI-mice, although transgenic mouse lines displayed differences in baseline performance as well as a progressive worsening (whose speed and extent was not affected by the traumatic lesion, either). In line with these observations, overall body weight profiles, disease onset and progression were not affected by the traumatic lesion in wt or in any of the transgenic lines (Suppl. Fig. 4). Likewise, survival of SOD1 and TDP-43 mice was not influenced by the traumatic lesion (data not shown).

4. Discussion

The pathogenesis of neurodegenerative conditions seems to be determined by the interaction of the genetic basis with a number of disparate environmental factors. Even though the number of genes associated with ALS is continuously growing, there is renewed attention to the non-genetic events that may trigger, accelerate or complicate the pathogenic process of ALS (Al-Chalabi and Pearce, 2015). It has been hypothesized that ALS onset may result from a multi-step chain of pathogenic events with up to 6 independent events (Al-Chalabi et al., 2014). However, the nature of the non-genetic events and how they interact with the genetic mutations remains elusive.

Brain trauma is considered as a risk factor for several neurodegenerative conditions. In fact, remote trauma increases the risk of Alzheimer's disease (Schofield et al., 1997) and lowers the age of onset of the disease (Nemetz et al., 1999). Similar effects have been described in Parkinson's disease (Goldman et al., 2006) and in Frontotemporal Dementia (Kalkonde et al., 2012). In ALS, traumatic brain injury may be involved as modifier of the onset or of the progression of the disease (Xi et al., 2014; Peters et al., 2013; Rosenbohm et al., 2014; Lehman

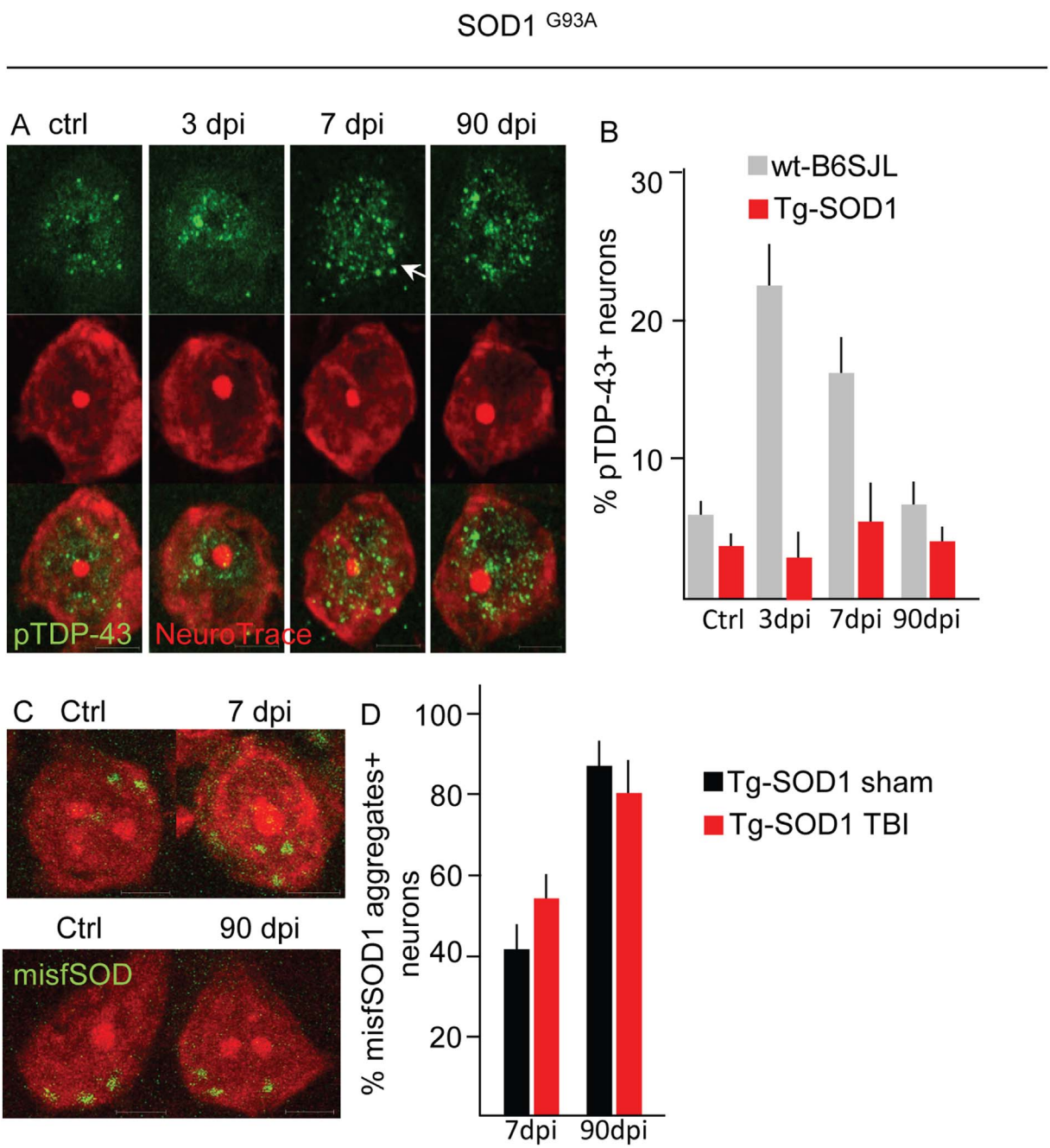

Fig. 5. (A) immunofluorescence images from layer V neurons of SOD1^{G93A} mice, 3, 7 and 90 dpi. No pTDP-43 granule appears in the SOD1^{G93A} mice upon stab injury to motor cortex. (B) Corresponding WT littermates shown upregulation of pTDP-43 granules upon trauma. Scale bar = 5 μm. (C) percentage of pTDP-43^{+} neurons in wildtype - (WT; B6SJL) and SOD1^{G93A} mice (SOD).

et al., 2012; Armon and Nelson, 2012). Furthermore, since TDP-43 proteinopathy has been hypothesized to propagate across neuronal networks (Braak et al., 2013), trauma-initiated ALS pathobiochemistry may actually act as a seed for disease initiation.

In order to elucidate the interaction between traumatic lesion of the motor cortex and specific vulnerability genotypes in shaping the appearance of ALS-related pathobiochemistry, we performed a highly reproducible, limited stab wound injury in the motor cortex of different strains of wt mice and mice carrying pathogenic mutations in TDP-43, FUS or SOD1.

As relevant readout, we analyzed the appearance of cytoplasmic granules of phosphorylated TDP-43 in neurons, which are related to the hallmark pathology of ALS and may be an intermediate step of the propagation itself in the "physical propagation" model (Braak et al., 2013). Notably, these granules do not seem to be part of stress granules, but, at least for a fraction, take part in complexes with the transport-granules protein FMRP. TDP-43/FMRP complexes have been previously reported (Majumder et al., 2016) to be involved in the repression of the translation of several cytoskeletal and synaptic proteins mRNA; therefore, the formation and the later clearance of the p-TDP-43 granules may be part of the cytoskeletal remodeling and regeneration that takes places after injury.

In the stab-injury model, the appearance of pTDP-43 granules was transient, going back to baseline after 40 dpi, implying that irrespective of the presence of genetic mutations in the TDP-43 molecule itself or in other ALS-related genes, the presence of cytoplasmic pTDP-43 granules is not an irreversible feature.

Interestingly, the kinetics of TDP-43 granules accumulation were

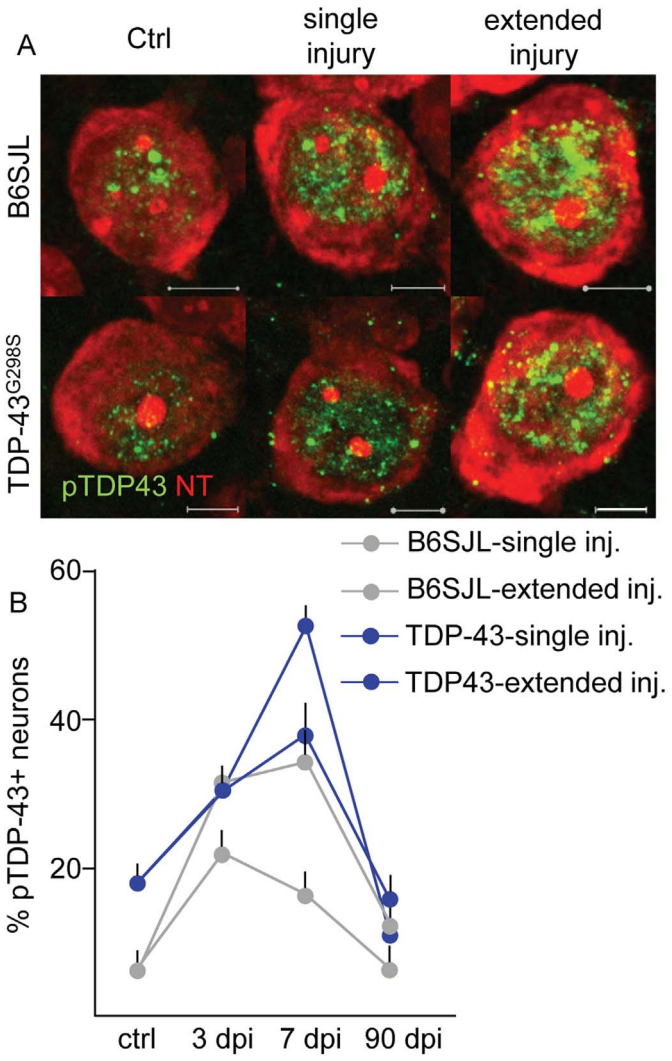

Fig. 6. (A–B) More severe lesion to motor cortex results in a larger number of neurons displaying pTDP-43 granules but not in a different kinetic of granules appearance compared to mild injury. Scale bar = 5 μm.

distinct in mice expressing wt TDP-43, mutant TDP-43 or mutant FUS. Mutant TDP-43 mice continued accumulating TDP-43 granules at 7 dpi whereas in wt TDP-43 mice the number of TDP-43 granules peaked at 3 dpi and were already declining at 7 dpi. Wt TDP-43 is normally cleared by the proteasome and by the autophagic pathway, with the latter being responsible of the degradation of aggregated TDP-43 (Scotter et al., 2014). In fact, the majority of pTDP-43 granules induced by the stab-injury was colocalized with the autophagy marker p62. Thus, it is conceivable that mutant TDP-43 mice, an imbalance between granule formation (mutant TDP-43 is, in fact, prone to aggregation; Guo et al., 2011) and clearance (which is itself regulated by TDP-43; Ying et al., 2016) may contribute to the continuing build-up of pTDP-43 granules at 7 dpi.

Furthermore, inflammation induces cytoplasmic TDP-43 translocation (Correia et al., 2015) and the enhanced astrocyte and leukocyte response observed in the mutant TDP-43 mice upon TBI may further increase the burden of pTDP-43 granules in neurons. Of note, in the mutant TDP-43 used for the present study, TDP-43^{G298S} was driven by the Thy1 promoter and therefore its expression was limited to neurons; thus, we hypothesize that the astrocyte phenotype is non-cell-autonomous and driven by pathogenic events unfolding in neurons. Although the role of TDP-43 in neuro-glial interaction in TBI has not been extensively investigated, TDP-43 has been reported to be essential for the processing of IL-6 and IL-10 and depletion of TDP-43 reduces IL-6 and IL-10 levels (Lee et al., 2015). Therefore, it is conceivable that mutant TDP-43 may enhance the neuroinflammatory response to trauma.

In mutant FUS mice, pTDP-43 granules only appear at 7 dpi (in a significantly larger number than in wt littermates). While the delayed appearance of pTDP-43 granules appears to be an effect of the background of the mice (C57BL/6 Tac in FUS mice vs B6SJL in SOD1 and TDP-43 mice), the effect of FUS on the autophagic pathway (Soo et al., 2015) may be involved in increasing the burden of pTDP-43 granules compared to wt littermates.

Surprisingly, SOD1 transgenic mice did not show any increase in pTDP-43^{+} neurons in response to stab wound injury. Although this finding is in line with the lack (or very late appearance) of pTDP-43 inclusions in SOD1 transgenic mice (Turner et al., 2008; Shan et al., 2009; Thomsen et al., 2014) or in human patients carrying mutations in the SOD1 gene (Mackenzie et al., 2007), it points out to a possible fundamental difference in TDP-43 biology in the context of SOD1 mutations. In particular, our findings are compatible with the recent evidence that mutant SOD1 may directly interfere with and delay the formation of stress granules (in which TDP-43 is a constituent) by sequestering fundamental GTPases and RNA-binding proteins (Gal et al., 2016).

Neuronal cell loss was not amplified by ALS-related genetic mutations, nor was the progression of disease in the TDP-43 and SOD1 mice influenced by the motor cortex lesion. Thus, cortical lesions can induce a limited and transient increase in cytoplasmic pTDP-43 levels in the form of granules, but this effect is neither intrinsically toxic to neurons nor affects the overall disease course.

With due caution, extrapolation of such findings to humans would imply that in patients at a genetic risk for ALS, a single, moderate trauma of the motor cortex may set in motion an initial translocation of TDP-43 to the cytoplasm which may revert to baseline unless additional factors affect it. Therefore, isolated brain trauma or neurosurgical procedures (such as diagnostic biopsies or therapeutic procedures) may confer only a small additional risk to these patients. An additional limitation of the present study is the detection of pTDP-43 granules only in the stab-injury model but not in the weight-drop TBI model. Thus, it is possible that pTDP-43 granules may appear only in case of significant disruption of the tissue, e.g. in case of extensive lesion to axons and dendrites. In fact, axotomy has been reported to be a substantial trigger for TDP-43 translocation after peripheral nerve injury (Moisse et al., 2009).

These findings suggest that the severity of the trauma, and the degree of tissue damage, may be modifiers of the potential link between TBI and ALS, and therefore these factors should be considered in the design of clinical studies on the subject. Furthermore, our data are in line with the clinical evidence which suggest that repeated trauma may be a severe risk factor in ALS than isolated traumatic events (Chen et al., 2007; Chiò et al., 2005). Since this study was limited to a single injury (although different severities were explored), caution should be used in extrapolating our observations to the effects of repeated traumas.

According to the propagation hypothesis, the effect of such “initiating lesion” may be higher in humans, who have monosynaptic connections between upper and lower motor neurons (whereas murine nervous systems largely lack such connections) that may provide a faster diffusion pathway for TDP-43 (Braak et al., 2013; Braak et al., 2016).

In a multi-event model, large population of affected neurons may be more at risk for additional disruptive events that may prevent the proper degradation of cytoplasmic TDP-43 granules. Thus, it is conceivable that acquired or genetic defects in autophagy (Freischmidt et al., 2015; Ciura et al., 2016) may worsen the cytoplasmic translocation of pTDP-43 by slowing down or preventing its degradation. In this framework, the pTDP-43 granules induced by trauma, may act as initiating lesions, enhanced by the presence of genetic risk factors

leading to dysfunction of other cellular pathways (TDP-43 itself, FUS, and autophagy).

Of note, inflammatory reaction following trauma may be an important regulator of this initiating step. In fact, inflammatory stimuli are sufficient to induce TDP-43 translocation to the cytoplasm (Correia et al., 2015). Loss-of-function mutations in the anti-inflammatory factor progranulin are linked to TDP-43-associated frontal cortical degeneration although additional genetic or environmental risk factors are thought to play a major role in determining their expressivity and penetrance (Petkau and Leavitt, 2014).

Thus, although a lesion in the motor cortex may trigger the temporary formation of a pool of neurons displaying cytoplasmic pTDP-43 granules (in all genotypes but mutant SOD1), this is not enough to produce long-term granules or overt degeneration, even in presence of ALS-related mutations in TDP-43, FUS or SOD1. In fact, no additional loss of layer V neurons was detected in the ALS-related line (compared to wt) and no difference in the rate of progression of motor impairment has been detected. Although a more subtle effect on MN loss cannot be discounted, the use of a behavioral, rather than histological criteria to define disease progression provides a direct assessment of the relevance of these data to human patients (while allowing the implementation of "3R" rules for animal experimentation). Thus, a multi-event model of ALS pathogenesis (Al-Chalabi and Hardiman, 2013; Al-Chalabi and Pearce, 2015) may be better suited to account for the interaction of genetic and environmental factors in the pathogenesis of ALS.

Supplementary data to this article can be found online at https://doi.org/10.1016/j.expneurol.2017.09.011.

Acknowledgement

F.R. is member of the Ulm Trauma Research Center and it is supported by DFG (SFB1149-B05) in the "Danger Response, Disturbance Factors and Regenerative Potential after Acute Trauma" Collaborative Research Center (SFB1149), by the ERANET-NEURON "External insults to the CNS" program as part of the MICRONET consortium and by the Baustein Program of the Ulm University Medical Faculty (LSBN108).

We are grateful to prof. Magdalena Goetz and prof. Leda Dimou for assistance in the trauma model. We thank prof. Frank Kirchhoff (Institute of Molecular Virology, Ulm University) for the use of the Zeiss 710 confocal microscope.

References

Al-Chalabi, A., Hardiman, O., 2013. The epidemiology of ALS: a conspiracy of genes, environment and time. Nat. Rev. Neurol. 9 (11), 617–628.

Al-Chalabi, A., Pearce, N., 2015. Commentary: mapping the human exposome: without it, how can we find environmental risk factors for ALS? Epidemiology 26 (6), 821–823.

Al-Chalabi, A., Calvo, A., Chio, A., Colville, S., Ellis, C.M., Hardiman, O., Heverin, M., Howard, R.S., Huisman, M.H., Keren, N., Leigh, P.N., Mazzini, L., Mora, G., Orrell, R.W., Rooney, J., Scott, K.M., Scotton, W.J., Seelen, M., Shaw, C.E., Sidle, K.S., Swingler, R., Tsuda, M., Veldink, J.H., Visser, A.E., van den Berg, L.H., Pearce, N., 2014. Analysis of amyotrophic lateral sclerosis as a multistep process: a population-based modelling study. Lancet Neurol. 13 (11), 1108–1113.

Armon, C., Nelson, L.M., 2012. Is head trauma a risk factor for amyotrophic lateral sclerosis? An evidence based review. Amyotroph. Lateral Scler. 13 (4), 351–356.

Braak, H., Brettschneider, J., Ludolph, A.C., Lee, V.M., Trojanowski, J.Q., Del Tredici, K., 2013. Amyotrophic lateral sclerosis—a model of corticofugal axonal spread. Nat. Rev. Neurol. 9 (12), 708–714.

Braak, H., Ludolph, A.C., Neumann, M., Ravits, J., Del Tredici, K., 2016. Pathological TDP-43 changes in Betz cells differ from those in bulbar and spinal α-motoneurons in sporadic amyotrophic lateral sclerosis. Acta Neuropathol. 18 (Epub ahead of print).

Brenner, D., Müller, K., Wieland, T., Weydt, P., Böhm, S., Lulé, D., Hübers, A., Neuwirth, C., Weber, M., Borck, G., Wahlqvist, M., Danzer, K.M., Volk, A.E., Meitinger, T., Strom, T.M., Otto, M., Kassubek, J., Ludolph, A.C., Andersen, P.M., Weishaupt, J.H., 2016. NEK1 mutations in familial amyotrophic lateral sclerosis. Brain 5 (pii: aww033).

Brettschneider, J., Del Tredici, K., Toledo, J.B., Robinson, J.L., Irwin, D.J., Grossman, M., Suh, E., Van Deerlin, V.M., Wood, E.M., Baek, Y., Kwong, L., Lee, E.B., Elman, L., McCluskey, L., Fang, L., Feldengut, S., Ludolph, A.C., Lee, V.M., Braak, H., Trojanowski, J.Q., 2013. Stages of pTDP-43 pathology in amyotrophic lateral sclerosis. Ann. Neurol. 74 (1), 20–38.

Brettschneider, J., Arai, K., Del Tredici, K., Toledo, J.B., Robinson, J.L., Lee, E.B., Kuwabara, S., Shibuya, K., Irwin, D.J., Fang, L., Van Deerlin, V.M., Elman, L., McCluskey, L., Ludolph, A.C., Lee, V.M., Braak, H., Trojanowski, J.Q., 2014. TDP-43 pathology and neuronal loss in amyotrophic lateral sclerosis spinal cord. Acta Neuropathol. 128 (3), 423–437.

Buffo, A., Rite, I., Tripathi, P., Lepier, A., Colak, D., Horn, A.P., Mori, T., Götz, M., 2008. Origin and progeny of reactive gliosis: a source of multipotent cells in the injured brain. Proc. Natl. Acad. Sci. U. S. A. 105 (9), 3581–3586.

Caller, T.A., Andrews, A., Field, N.C., Henegan, P.L., Stommel, E.W., 2015. The epidemiology of amyotrophic lateral sclerosis in New Hampshire, USA, 2004–2007. Neurodegener. Dis. 15 (4), 202–206.

Chen, H., Richard, M., Sandler, D.P., Umbach, D.M., Kamel, F., 2007. Head injury and amyotrophic lateral sclerosis. Am. J. Epidemiol. 166 (7), 810–816.

Chiò, A., Benzi, G., Dossena, M., Mutani, R., Mora, G., 2005. Severely increased risk of amyotrophic lateral sclerosis among Italian professional football players. Brain 128 (Pt 3), 472–476.

Ciura, S., Sellier, C., Campanari, M.L., Charlet-Berguerand, N., Kabashi, E., 2016. The most prevalent genetic cause of ALS-FTD, C9orf72 synergizes the toxicity of ATXN2 intermediate polyglutamine repeats through the autophagy pathway. Autophagy 12 (8), 1406–1408.

Correia, A.S., Patel, P., Dutta, K., Julien, J.P., 2015. Inflammation induces TDP-43 mislocalization and aggregation. PLoS One 10 (10), e0140248. http://dx.doi.org/10.1371/journal.pone.0140248.

Couratier, P., Corcia, P., Lautrette, G., Nicol, M., Preux, P.M., Marin, B., 2016. Epidemiology of amyotrophic lateral sclerosis: a review of literature. Rev. Neurol. (Paris) 172 (1), 37–45.

Coyne, A.N., Yamada, S.B., Siddegowda, B.B., Estes, P.S., Zaepfel, B.L., Johannesmeyer, J.S., Lockwood, D.B., Pham, L.T., Hart, M.P., Cassel, J.A., Freibaum, B., Boehringer, A.V., Taylor, J.P., Reitz, A.B., Gitler, A.D., Zarnescu, D.C., 2015. Fragile X protein mitigates TDP-43 toxicity by remodeling RNA granules and restoring translation. Hum. Mol. Genet. 24 (24), 6886–6898.

Dewey, C.M., Cenik, B., Sephton, C.F., Dries, D.R., Mayer 3rd, P., Good, S.K., Johnson, B.A., Herz, J., Yu, G., 2011. TDP-43 is directed to stress granules by sorbitol, a novel physiological osmotic and oxidative stressor. Mol. Cell. Biol. 31 (5), 1098–1108.

Dictenberg, J.B., Swanger, S.A., Antar, L.N., Singer, R.H., Bassell, G.J., 2008. A direct role for FMRP in activity-dependent dendritic mRNA transport links filopodial-spine morphogenesis to fragile X syndrome. Dev. Cell 14 (6), 926–939.

Flierl, M.A., Stahel, P.F., Beauchamp, K.M., Morgan, S.J., Smith, W.R., Shohami, E., 2009. Mouse closed head injury model induced by a weight-drop device. Nat. Protoc. 4 (9), 1328–1337.

Fournier, C.N., Gearing, M., Upadhyayula, S.R., Klein, M., Glass, J.D., 2015. Head injury does not alter disease progression or neuropathologic outcomes in ALS. Neurology 84 (17), 1788–1795.

Freischmidt, A., Wieland, T., Richter, B., Ruf, W., Schaeffer, V., Müller, K., Marroquin, N., Nordin, F., Hübers, A., Weydt, P., Pinto, S., Press, R., Millecamps, S., Molko, N., Bernard, E., Desnuelle, C., Soriani, M.H., Dorst, J., Graf, E., Nordström, U., Feiler, M.S., Putz, S., Boeckers, T.M., Meyer, T., Winkler, A.S., Winkelman, J., de Carvalho, M., Thal, D.R., Otto, M., Brännström, T., Volk, A.E., Kursula, P., Danzer, K.M., Lichtner, P., Dikic, I., Meitinger, T., Ludolph, A.C., Strom, T.M., Andersen, P.M., Weishaupt, J.H., 2015. Haploinsufficiency of TBK1 causes familial ALS and fronto-temporal dementia. Nat. Neurosci. 18 (5), 631–636.

Gal, J., Kuang, L., Barnett, K.R., Zhu, B.Z., Shissler, S.C., Korotkov, K.V., Hayward, L.J., Kasarskis, E.J., Zhu, H., 2016. ALS mutant SOD1 interacts with G3BP1 and affects stress granule dynamics. Acta Neuropathol. 132 (4), 563–576.

Goldman, S.M., Tanner, C.M., Oakes, D., Bhudhikanok, G.S., Gupta, A., Langston, J.W., 2006. Head injury and Parkinson's disease risk in twins. Ann. Neurol. 60 (1), 65–72.

Guo, W., Chen, Y., Zhou, X., Kar, A., Ray, P., Chen, X., Rao, E.J., Yang, M., Ye, H., Zhu, L., Liu, J., Xu, M., Yang, Y., Wang, C., Zhang, D., Bigio, E.H., Mesulam, M., Shen, Y., Xu, Q., Fushimi, K., Wu, J.Y., 2011. An ALS-associated mutation affecting TDP-43 enhances protein aggregation, fibril formation and neurotoxicity. Nat. Struct. Mol. Biol. 18 (7), 822–830.

Gurney, M.E., Pu, H., Chiu, A.Y., Dal Canto, M.C., Polchow, C.Y., Alexander, D.D., Caliendo, J., Hentati, A., Kwon, Y.W., Deng, H.X., 1994. Motor neuron degeneration in mice that express a human Cu,Zn superoxide dismutase mutation. Science 264 (5166), 1772–1775.

Gyoneva, S., Kim, D., Katsumoto, A., Kokiko-Cochran, O.N., Lamb, B.T., Ransohoff, R.M., 2015. Ccr2 deletion dissociates cavity size and tau pathology after mild traumatic brain injury. J. Neuroinflammation 12, 228.

Hübers, A., Just, W., Rosenbohm, A., Müller, K., Marroquin, N., Goebel, I., Högel, J., Thiele, H., Altmüller, J., Nürnberg, P., Weishaupt, J.H., Kubisch, C., Ludolph, A.C., Volk, A.E., 2015. De novo FUS mutations are the most frequent genetic cause in early-onset German ALS patients. Neurobiol. Aging 36 (11) (3117.e1-6).

Johnson, V.E., Stewart, W., Trojanowski, J.Q., Smith, D.H., 2011. Acute and chronically increased immunoreactivity to phosphorylation-independent but not pathological TDP-43 after a single traumatic brain injury in humans. Acta Neuropathol. 122 (6), 715–726.

Kalkonde, Y.V., Jawaid, A., Qureshi, S.U., Shirani, P., Wheaton, M., Pinto-Patarroyo, G.P., Schulz, P.E., 2012. Medical and environmental risk factors associated with fronto-temporal dementia: a case-control study in a veteran population. Alzheimers Dement. 8 (3), 204–210.

Lee, S., Lee, T.A., Lee, E., Kang, S., Park, A., Kim, S.W., Park, H.J., Yoon, J.H., Ha, S.J., Park, T., Lee, J.S., Cheon, J.H., Park, B., 2015. Identification of a subnuclear body involved in sequence-specific cytokine RNA processing. Nat. Commun. 6, 5791.

Lehman, E.J., Hein, M.J., Baron, S.L., Gersic, C.M., 2012. Neurodegenerative causes of death among retired National Football League players. Neurology 79 (19), 1970–1974.

Mackenzie, I.R., Bigio, E.H., Ince, P.G., Geser, F., Neumann, M., Cairns, N.J., Kwong, L.K.,

Forman, M.S., Ravits, J., Stewart, H., Eisen, A., McClusky, L., Kretzschmar, H.A., Monoranu, C.M., Highley, J.R., Kirby, J., Siddique, T., Shaw, P.J., Lee, V.M., Trojanowski, J.Q., 2007. Pathological TDP-43 distinguishes sporadic amyotrophic lateral sclerosis from amyotrophic lateral sclerosis with SOD1 mutations. Ann. Neurol. 61 (5), 427–434.

Majumder, P., Chu, J.F., Chatterjee, B., Swamy, K.B., Shen, C.J., 2016. Co-regulation of mRNA translation by TDP-43 and Fragile X Syndrome protein FMRP. Acta Neuropathol. 132 (5), 721–738.

McKee, A.C., Gavett, B.E., Stern, R.A., Nowinski, C.J., Cantu, R.C., Kowall, N.W., Perl, D.P., Hedley-Whyte, E.T., Price, B., Sullivan, C., Morin, P., Lee, H.S., Kubilus, C.A., Daneshvar, D.H., Wulff, M., Budson, A.E., 2010. TDP-43 proteinopathy and motor neuron disease in chronic traumatic encephalopathy. J. Neuropathol. Exp. Neurol. 69 (9), 918–929.

Moisse, K., Volkening, K., Leystra-Lantz, C., Welch, I., Hill, T., Strong, M.J., 2009. Divergent patterns of cytosolic TDP-43 and neuronal progranulin expression following axotomy: implications for TDP-43 in the physiological response to neuronal injury. Brain Res. 1249, 202–211.

Nemetz, P.N., Leibson, C., Naessens, J.M., Beard, M., Kokmen, E., Annegers, J.F., Kurland, L.T., 1999. Traumatic brain injury and time to onset of Alzheimer's disease: a population-based study. Am. J. Epidemiol. 149 (1), 32–40.

Neumann, M., Kwong, L.K., Lee, E.B., Kremmer, E., Flatley, A., Xu, Y., Forman, M.S., Troost, D., Kretzschmar, H.A., Trojanowski, J.Q., Lee, V.M., 2009. Phosphorylation of S409/410 of TDP-43 is a consistent feature in all sporadic and familial forms of TDP-43 proteinopathies. Acta Neuropathol. 117 (2), 137–149.

Peters, T.L., Fang, F., Weibull, C.E., Sandler, D.P., Kamel, F., Ye, W., 2013. Severe head injury and amyotrophic lateral sclerosis. Amyotroph. Lateral Scler Frontotemporal Degener. 14 (4), 267–272.

Petkau, T.L., Leavitt, B.R., 2014. Progranulin in neurodegenerative disease. Trends Neurosci. 37 (7), 388–398.

Philips, T., Robberecht, W., 2011. Neuroinflammation in amyotrophic lateral sclerosis: role of glial activation in motor neuron disease. Lancet Neurol. 10 (3), 253–263.

Pickles, S., Destroismaisons, L., Peyrard, S.L., Cadot, S., Rouleau, G.A., Brown Jr., R.H., Julien, J.P., Arbour, N., Vande, Velde C., 2013. Mitochondrial damage revealed by immunoselection for ALS-linked misfolded SOD1. Hum. Mol. Genet. 22 (19), 3947–3959.

van Putten, M., de Winter, C., van Roon-Mom, W., van Ommen, G.J., t Hoen PA, Aartsma-Rus A., 2010. A 3 months mild functional test regime does not affect disease parameters in young mdx mice. Neuromuscul. Disord. 20 (4), 273–280. http://dx.doi.org/10.1016/j.nmd.2010.02.004. (Epub 2010 Mar 21).

Riva, N., Agosta, F., Lunetta, C., Filippi, M., Quattrini, A., 2016. Recent advances in amyotrophic lateral sclerosis. J. Neurol. 30.

Rosenbohm, A., Kassubek, J., Weydt, P., Marroquin, N., Volk, A.E., Kubisch, C., Huppertz, H.J., Weber, M., Andersen, P.M., Weishaupt, J.H., Ludolph, A.C., ALS Schwaben Register Group, 2014. Can lesions to the motor cortex induce amyotrophic lateral sclerosis? J. Neurol. 261 (2), 283–290.

Scekic-Zahirovic, J., Sendscheid, O., El Oussini, H., Jambeau, M., Sun, Y., Mersmann, S., Wagner, M., Dieterlé, S., Sinniger, J., Dirrig-Grosch, S., Drenner, K., Birling, M.C., Qiu, J., Zhou, Y., Li, H., Fu, X.D., Rouaux, C., Shelkovnikova, T., Witting, A., Ludolph, A.C., Kiefer, F., Storkebaum, E., Lagier-Tourenne, C., Dupuis, L., 2016. Toxic gain of function from mutant FUS protein is crucial to trigger cell autonomous motor neuron loss. EMBO J. 35 (10), 1077–1097.

Schofield, P.W., Tang, M., Marder, K., Bell, K., Dooneief, G., Chun, M., Sano, M., Stern, Y., Mayeux, R., 1997. Alzheimer's disease after remote head injury: an incidence study. J. Neurol. Neurosurg. Psychiatry 62 (2), 119–124.

Scotter, E.L., Vance, C., Nishimura, A.L., Lee, Y.B., Chen, H.J., Urwin, H., Sardone, V., Mitchell, J.C., Rogelj, B., Rubinsztein, D.C., Shaw, C.E., 2014. Differential roles of the ubiquitin proteasome system and autophagy in the clearance of soluble and aggregated TDP-43 species. J. Cell Sci. 127 (Pt 6), 1263–1278.

Shan, X., Vocadlo, D., Krieger, C., 2009. Mislocalization of TDP-43 in the G93A mutant SOD1 transgenic mouse model of ALS. Neurosci. Lett. 458 (2), 70–74.

Shan, X., Chiang, P.M., Price, D.L., Wong, P.C., 2010. Altered distributions of Gemini of coiled bodies and mitochondria in motor neurons of TDP-43 transgenic mice. Proc. Natl. Acad. Sci. U. S. A. 107 (37), 16325–16330.

Simon, C., Götz, M., Dimou, L., 2011. Progenitors in the adult cerebral cortex: cell cycle properties and regulation by physiological stimuli and injury. Glia 59 (6), 869–881.

Soo, K.Y., Sultana, J., King, A.E., Atkinson, R., Warraich, S.T., Sundaramoorthy, V., Blair, I., Farg, M.A., Atkin, J.D., 2015. ALS-associated mutant FUS inhibits macroautophagy which is restored by overexpression of Rab1. Cell Death Dis. 1, 15030.

Steinberg, K.M., Yu, B., Koboldt, D.C., Mardis, E.R., Pamphlett, R., 2015. Exome sequencing of case-unaffected-parents trios reveals recessive and de novo genetic variants in sporadic ALS. Sci Rep 5, 9124.

Thomsen, G.M., Gowing, G., Latter, J., Chen, M., Vit, J.P., Staggenborg, K., Avalos, P., Alkaslasi, M., Ferraiuolo, L., Likhite, S., Kaspar, B.K., Svendsen, C.N., 2014. Delayed disease onset and extended survival in the SOD1G93A rat model of amyotrophic lateral sclerosis after suppression of mutant SOD1 in the motor cortex. J. Neurosci. 34 (47), 15587–15600.

Turner, B.J., Bäumer, D., Parkinson, N.J., Scaber, J., Ansorge, O., Talbot, K., 2008. TDP-43 expression in mouse models of amyotrophic lateral sclerosis and spinal muscular atrophy. BMC Neurosci. 9, 104.

Urwin, H., Josephs, K.A., Rohrer, J.D., Mackenzie, I.R., Neumann, M., Authier, A., Seelaar, H., Van Swieten, J.C., Brown, J.M., Johannsen, P., Nielsen, J.E., Holm, I.E., FReJA Consortium, Dickson, D.W., Rademakers, R., Graff-Radford, N.R., Parisi, J.E., Petersen, R.C., Hatanpaa, K.J., White 3rd, C.L., Weiner, M.F., Geser, F., Van Deerlin, V.M., Trojanowski, J.Q., Miller, B.L., Seeley, W.W., van der Zee, J., Kumar-Singh, S., Engelborghs, S., De Deyn, P.P., Van Broeckhoven, C., Bigio, E.H., Deng, H.X., Halliday, G.M., Kril, J.J., Munoz, D.G., Mann, D.M., Pickering-Brown, S.M., Doodeman, V., Adamson, G., Ghazi-Noori, S., Fisher, E.M., Holton, J.L., Revesz, T., Rossor, M.N., Collinge, J., Mead, S., Isaacs, A.M., 2010. FUS pathology defines the majority of tau- and TDP-43-negative frontotemporal lobar degeneration. Acta Neuropathol. 120 (1), 33–41.

Valavanis, A., Schwarz, U., Baumann, C.R., Weller, M., Linnebank, M., 2014. Amyotrophic lateral sclerosis after embolization of cerebral arterioveneous malformations. J. Neurol. 261 (4), 732–737.

Wang, H.K., Lee, Y.C., Huang, C.Y., Liliang, P.C., Lu, K., Chen, H.J., Li, Y.C., Tsai, K.J., 2015. Traumatic brain injury causes frontotemporal dementia and TDP-43 proteolysis. Neuroscience 300, 94–103.

Xi, Z., Yunusova, Y., van Blitterswijk, M., Dib, S., Ghani, M., Moreno, D., Sato, C., Liang, Y., Singleton, A., Robertson, J., Rademakers, R., Zinman, L., Rogaeva, E., 2014. Identical twins with the C9orf72 repeat expansion are discordant for ALS. Neurology 83 (16), 1476–1478.

Ying, Z., Xia, Q., Hao, Z., Xu, D., Wang, M., Wang, H., Wang, G., 2016. TARDBP/TDP-43 regulates autophagy in both MTORC1-dependent and MTORC1-independent manners. Autophagy 4, 707–708.